CCUS: 4014596

The effect of natural fractures on CO_2 injection and storage capacity in tight sandstone reservoir, St. Lawrence Platform, Quebec

Elena Konstantinovskaya[1], Jean-Sébastien Marcil*[2], Jose Rivero[3], Valentina Vallega[3],
1. University of Alberta. 2, Utica Resources. 3, SLB.

This paper was prepared for presentation at the Carbon Capture, Utilization, and Storage conference held in Houston, TX, 11-13 March.

Abstract

The analysis of outcrops and image logs in vertical and horizontal wells was conducted in Lower Paleozoic sedimentary succession of the St. Lawrence Platform, Quebec to characterize the type, orientation, and distribution of natural fractures in reservoir and overlying caprock units. The obtained results were applied in DFN modeling to take into account the presence of natural fractures in the mechanically heterogeneous sedimentary succession. 3D reservoir-geomechanical modeling of CO_2 injection was carried out in a deep saline aquifer of the tight fractured reservoir of the Potsdam sandstone at a depth of ~1.2 km to study the effect of natural fractures on CO_2 injection and storage capacity and risk of seal failure. Based on these results obtained in the Bécancour industrial sector, a geologically well-known region, we evaluate the geological storage potential of two other less explored industrial sectors of the St. Lawrence Platform.

Introduction

CO_2 storage operations in tight sandstone reservoirs require an understanding of the subsurface system of natural fractures in the reservoir and caprock. The deep saline aquifers of the Potsdam Group of Lower Paleozoic sedimentary succession of the St. Lawrence Platform represent one of the main potential targets for CO_2 sequestration in Quebec Province (Malo and Bédard, 2012; Tran Ngoc et al., 2014).

The Potsdam Group is composed of Cambrian-Lower Ordovician sandstone of the basal Covey Hill and overlying Cairnside Formations. The Covey Hill Formation is composed of basal red-color mostly fluvial quartz-feldspar sandstone to conglomerate overlying with discordance the Grenvillian metamorphic basement (Globensky, 1987). It may contain thin dolomitic beds. The Cairnside Formation consists of white to grey tide-dominated shallow marine pure quartz sandstone (Lewis, 1971; Globensky, 1987; Salad Hersi and Lavoie, 2000). The overlying Ordovician tight carbonate rocks of the Beekmantown and

Trenton Group, Utica Shale, and Lorraine Group, if not fractured, are generally tight and provide a thick top seal above the reservoir. The Potsdam sandstone and Beekmantown limestone and dolomite were accumulated under the settings of the Cambrian-Ordovician rift and passive margin. The overlying Middle to Upper Ordovician units were deposited in a foreland basin setting (Globensky, 1987; Lavoie, 1994). The metamorphic and igneous rocks of the Grenvillian basement form a bottom seal below the reservoir.

The St. Lawrence Platform sedimentary basin is extended for about 200 km from Montreal in the SW to Quebec City in the NE, separating the Grenvillian basement in the NW and the Appalachian orogenic belt in the SE. The numerous longitudinal normal faults dipping to the NW and SE displace the top of the Grenvillian basement and Lower Paleozoic sedimentary succession of the St. Lawrence Platform (Castonguay et al., 2010). The Yamaska Fault is one of the major normal faults present in the study area (Figure 1). Basement normal faults in the St Lawrence Platform were initiated in the Neoproterozoic during rifting and extension of the Laurentian continental margin and opening of the Iapetus Ocean (Cawood et al., 2001; Hibbard et al., 2007; O'Brien and van der Pluijm, 2012). Some of these faults were subsequently and repetitively reactivated as synsedimentary normal faults during the middle–late Ordovician, late Silurian–early Devonian, and in the early Jurassic (St-Julien and Hubert, 1975; Séjourné et al., 2003; Tremblay et al., 2007). The autochthonous sedimentary units of the St. Lawrence Platform are folded in the regional wide, open Chambly-Fortierville syncline delineated in the SE by the triangle zone and the NW-verging thrusts of the parautochthonous domain and Appalachian allochthonous domain formed during the Taconian Orogeny (St-Julien and Hubert, 1975; Globensky, 1987; Konstantinovskaya et al., 2009; Castonguay et al., 2010).

A few sets of lineaments were interpreted in the St. Lawrence Platform based on the interpretation of the Landsat satellite images in the area (Konstantinovskaya et al., 2012). The more numerous and longer lineaments are oriented NE–SW rotating to NNE–SSW in the Montreal area. These lineaments reflect the principal structural pattern of the regional normal and thrust faults. The lineaments of NNW–SSE and WNW–ESE directions are shorter and less numerous than the first set. Fractures in the Utica Shale are generally oriented NE-SW and NW-SE, as interpreted from the satellite image of the north and south shore of the St. Lawrence River (Pinet, 2011). The distribution of natural fractures was studied in the siltstone units of the Lorraine Group and the Utica Shale in the St. Edouard area, located at ~65 km to the SW of Quebec City. The fractures in these units form three main sets, oriented NE-SW, NW-SE, and WNW-ESE (Ladevèze et al., 2018). Natural fractures in sedimentary units of the St. Lawrence Platform could have been formed during the different phases of deformation, including the phases of a passive margin and foreland basin (Pinet, 2011), or, to some extent, related to the state of the present-day stress field (Konstantinovskaya et al., 2012).

The study area is located near Bécancour (Figure 1), in the footwall of the Yamaska Fault, in the central part of the St. Lawrence Platform. The area has been explored for hydrocarbon and gas storage since 1970 and around twenty wells were drilled there.

The previous 2D and 3D coupled reservoir-geomechanical simulation of CO_2 injection in a deep saline aquifer of the Potsdam sandstone was carried out in the Bécancour area at a depth of ~1.2 km (Figure 1) to study CO_2 injectivity and risk of fault reactivation and seal failure (Konstantinovskaya et al., 2014, 2020). The 3D simulation of CO_2 injection in the Potsdam aquifer was conducted in the Gentilly area at a depth of ~2.4-2.5 km (Konstantinovskaya et al., 2023). The evaluation of hydrogeological impacts of CO_2 injection, such as pore pressure buildup and brine leakage, was studied at the basin scale in the St. Lawrence Platform (Girou, 2017).

However, no modeling of CO_2 injection in the tight sandstone reservoir with natural fractures was previously carried out in the region.

Methods

The data for seven of wells (Figure 1) were used in this study. The data extracted from drilling sampling, DST, conventional, and image logs made it possible to determine the reservoir characteristics of the Bécancour sector and to carry out several injection simulations.

Petrophysical properties (porosity and permeability) of the Potsdam sandstone were derived from well logs and calibrated with core petrophysical testing data. The permeability curve was derived from the total porosity curve using the porosity-permeability correlation established based on core petrophysical testing data.

The analysis of image logs recorded in three vertical wells (A246, 247, 262) in the Bécancour area (Figure 1) and one horizontal well in the Gentilly area (16 km to the east from the Bécancour area) was used to characterize type, orientation, and frequency of natural and drilling induced fractures and borehole breakouts in different sedimentary units. The analyzed intervals involved Utica Shale, Trenton, Beekmantown, and Potsdam (Cairnside Formation) Groups.

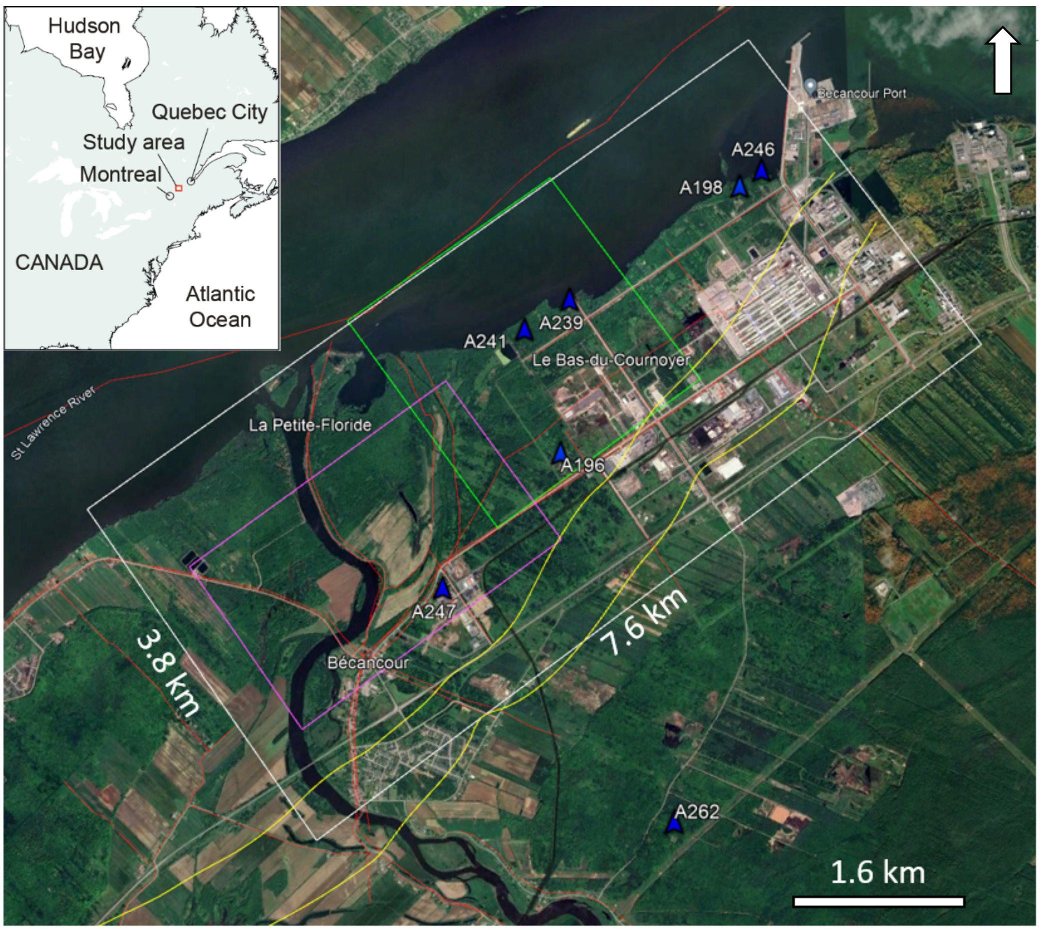

Figure 1. Location of structural (3.8 km x 7.6 km, white polygon) and reservoir simulation (2.4 km x 2.5 km green polygon) models in the Bécancour area projected on the Google Earth map. Red lines and pink polygon indicate location of 2D and 3D seismic surveys, respectively. Blue triangles indicate location of the wells used in this study. The SW-NE striking yellow lines correspond to the footwall and hanging wall limits of the Yamaska Fault at the top of the Covey Hill Formation.

The fracture frequency was estimated in TECHLOG based on the interpretation of the FMI log in the horizontal well in the Utica Shale. Additionally, the orientation of discontinuity lineaments was interpreted in PETREL^{TM} by applying the ant-tracking workflow to the 3D amplitude cube (Figure 1). The natural fractures were also observed and analyzed in outcrop analogs of the sedimentary units of the St. Lawrence Platform area.

3D structural modeling Discrete Fracture Network (DFN) modeling was completed in PETREL^{TM} using available well data and interpretation of 2D (Claprood et al., 2012) and 3D seismic data (Figure 1) in the Bécancour area. The porosity and permeability properties in the Potsdam sandstone were upscaled from logs in wells A196, and A198 and propagated in the model using kriging and Gaussian geostatistical methods.

3D reservoir simulations of CO_2 injection in the saline aquifers of the Potsdam sandstone were conducted for 20 years from January 2023 to January 2043 in ECLIPSE300 using the CO2STORE module. The cases of single porosity, dual porosity, and dual permeability were considered to take into account the fluid flow in natural fractures. The history of salt-water production from deep saline aquifers was available in wells A198 and A239 (Junex, 2018; Ressources Utica, 2020).

3D coupled reservoir-geomechanical simulations were conducted in VISAGE^{TM} to model pore pressure and present-day principal stresses and analyze the risk of top seal failure and fault/fracture reactivation.

Results

1. Petrophysical analysis

The sandstone of the Cairnside Formation is characterized by lower total porosity and permeability than the underlying Covey Hill sandstone (Figure 2). The core matrix porosity and permeability range from 0.10-3.9% and 0.02-0.52 mD in the Cairnside Formation to 3.9-13% and 0.13-4.3 mD in the Covey Hill Formation. The log-derived total porosity and permeability vary from 1.8-3% and 0.03-0.1 mD in the Cairnside Formation to 5-8% and 0.3-2 mD up to ~10 mD in the Covey Hill Formation. Low porosity and permeability of the Potsdam sandstone is compensated by considerable thickness reaching about 100 m in the Cairnside Formation and ~200 m in the Covey Hill Formation in the study area (Figure 2).

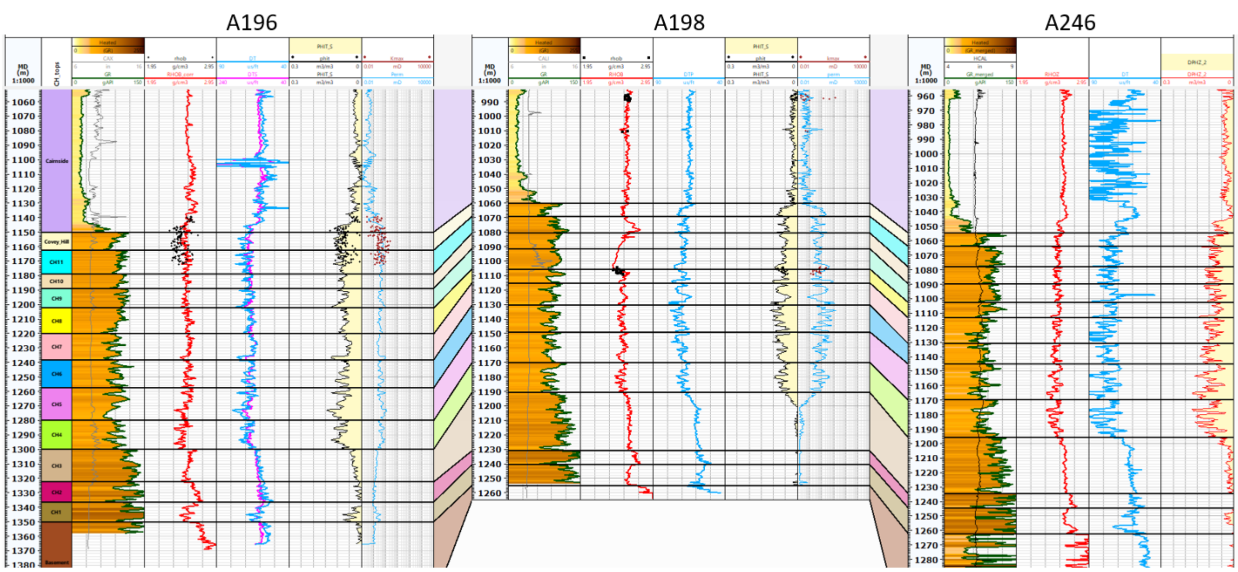

Figure 2. Well section showing well logs of GR, caliper (CAX); bulk density (RHOB); sonic logs (DT, DTS); total sonic (PHIT_S) and density (DPHZ) porosity and permeability (perm) and calibration points of petrophysical core testing data in wells A196, A198 and A246 in the study area (Figure 1). The 12 units in the Covey Hill Formation (CH1-CH12) are correlated between the wells.

According to the DST tests, permeability may increase up to 15.6 mD in the Cairnside sandstone (well A158), and it may be as high as 24.5 mD in the dolomitic rocks of the Beekmantown Group and 234 mD in the limestone of the Trenton Group (well A198). These high permeability values support the presence of fractures both in the Potsdam reservoir and in the overlying formations.

2. Fracture Analysis based on image logs

The FMI interpretation of natural fractures is available in wells A246 and A262 located in the footwall and the hanging wall of the Yamaska Fault, respectively. The fractures in the Cairnside Formation are available only in A246 well (Figure 3). The fracture interpretation data in well A262 are available in the intervals of the Utica Shale, Trenton, and Beekmantown Groups.

Bedding in the vertical well A246 is subhorizontal, dipping to the W at a very low angle (mean Dip Azimuth N275°, Dip Angle 5°). A total count of 7 conductive fractures and 17 partially conductive fractures and 3 healed fractures was interpreted in the interval of ~200 m. The mean Dip Azimuth is N108.3°/Dip angle 80° for the conductive fractures, N214.4°/40° and N109.3°/55° for the partially conductive fractures, and N143.7°/46°, N80.8°/60° and N16.7°/66° for the healed fractures.

The analysis of FMI logs in the study area indicates the presence of two main sets of natural fractures with mean Dip Azimuth N108°, Dip Angle 80° and N214°/40°. The NE-SW and NW-SE orientation of these two sets is similar to the orientation of fracture sets established for the siltstones of the Lorraine Group and Utica Shale (Pinet, 2011; Ladevèze et al., 2018). The analysis of ant-tracking volume revealed the presence of discontinuity lineaments in the Covey Hill Formation, which are 480-700 m long striking N18°E and N72°E. The first set of lineaments is parallel to conductive natural fractures identified in the image logs in the Cairnside Formation and Utica Shale. However, given the relatively poor quality of the 3D amplitude volume, these data should be considered cautiously.

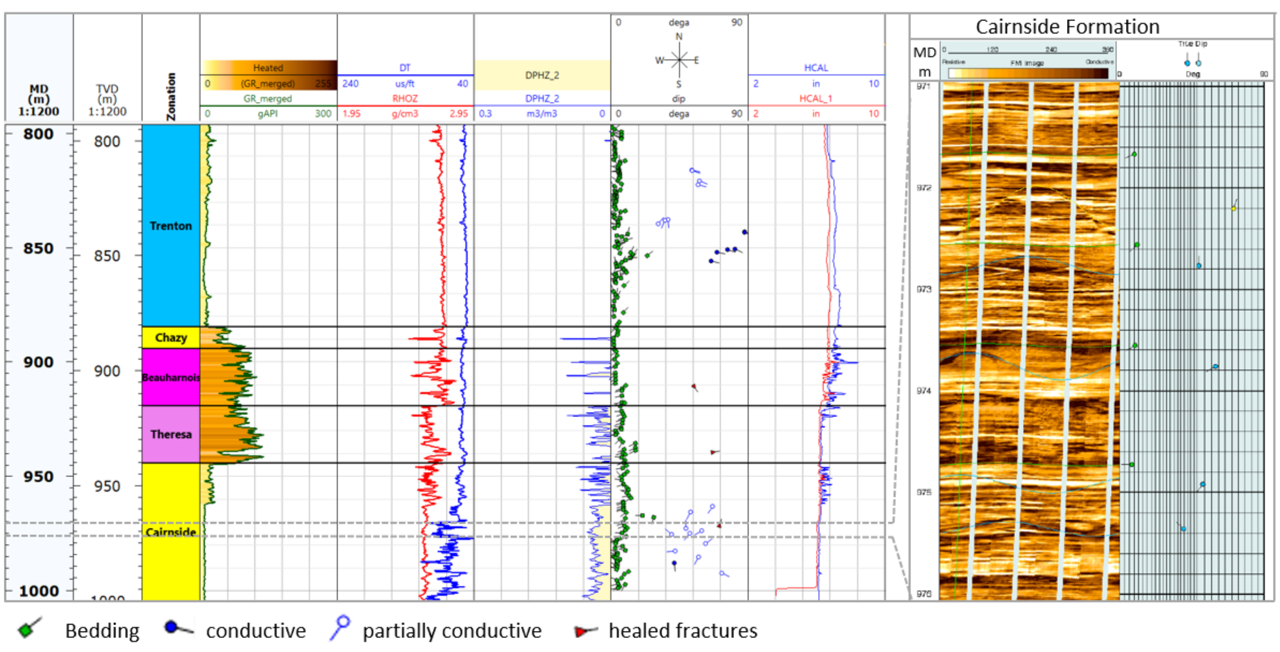

Figure 3. Log plot for well A246 displaying well logs GR, bulk density (RHOZ), P-sonic (DT), density porosity (DPHZ), FMI interpretation of bedding (green filled squares), conductive (blue filled circles), partially conductive (blue open circles) and healed (red triangles) fractures. Interval of FMI log in the Cairnside sandstone displays bedding (green circles), partially open (blue circles) and healed (yellow circles) fractures.

3. 3D reservoir simulations

3D reservoir simulations of CO_2 injection in the saline aquifer of the Potsdam sandstone were conducted in the area of 2.4 km x 2.5 km with injection simulation in vertical well Inj3_A247vert, located near well A247, in the area of relative uplift in the top of the Potsdam sandstone (Figure 4).

Four perforations were designed in the completion of the well located at the depth intervals of higher porosity and permeability (Figure 4). 3D reservoir simulations were conducted for the cases with single matrix porosity, dual porosity, and dual permeability to take into account the presence of natural fractures.

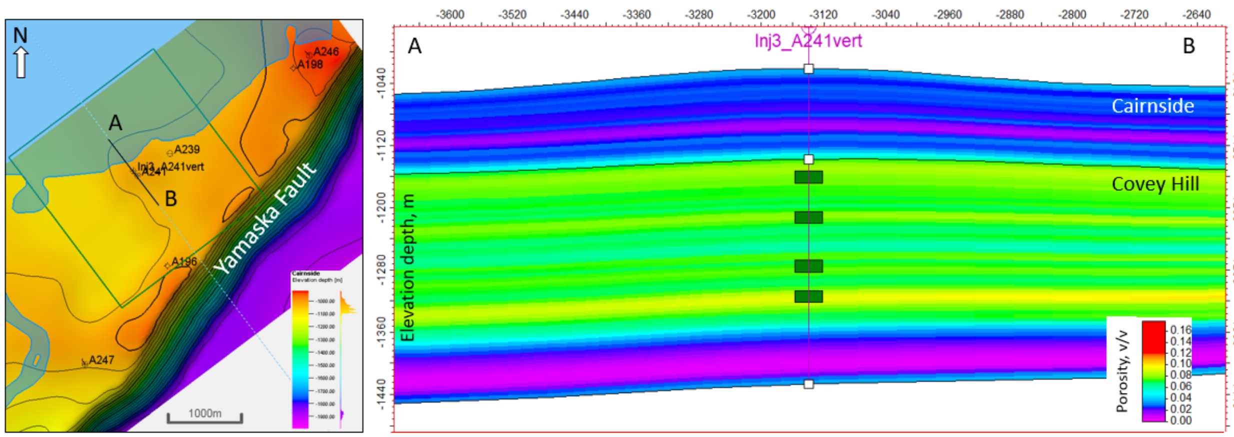

Figure 4. Structural map of the top of the Cairnside Formation in the footwall of the Yamaska Fault (on the left) and distribution of the property of total porosity (PHIT) of the Potsdam sandstone along the cross-section A-B, VE=1 (on the right). The PHIT and permeability well logs in wells A196 and A198 (Figure 2) were upscaled and propagated using kriging method in 3D reservoir simulation model (green polygon). Location of injection well Inj3_wellA241vert and designed perforations are shown.

The case studies presented below describe the results of 3D reservoir simulations conducted in the Bécancour area (Figure 4) for 20 years from January 2023 to January 2043.

Case 1. Single matrix porosity.

The CO_2 injection was conducted under settings of matrix porosity and permeability upscaled from the well log data calibrated by core data (Figure 2). The sandstone of the Cairnside Formation was more tight than the sandstone of the Covey Hill Formation. The CO_2 was injected into the injection well at a rate of 0.5 kg/s (23117.7 Sm3/day or 15.8 kt/a), which allowed continuous injection over 14 years (July 15, 2037) without reaching the upper limit of the borehole pressure (BHP) of 20.8 MPa (208 bar). The upper BHP limit corresponds to the value of the total minimum horizontal stress at the top of the Potsdam sandstone that was used to minimize the risk of tensile failure in the injection well or in the top cap rock. After reaching the upper BHP limit, the injection continued to Jan 2043 at a lower injection rate (Figure 5).

The gas injection cumulative was 287.7 kt after 20 years of injection in one well. The CO_2 plume was symmetrical with a diameter of 375 m and a height of 244 m, mainly contained in the Covey Hill Formation (Figure 6).

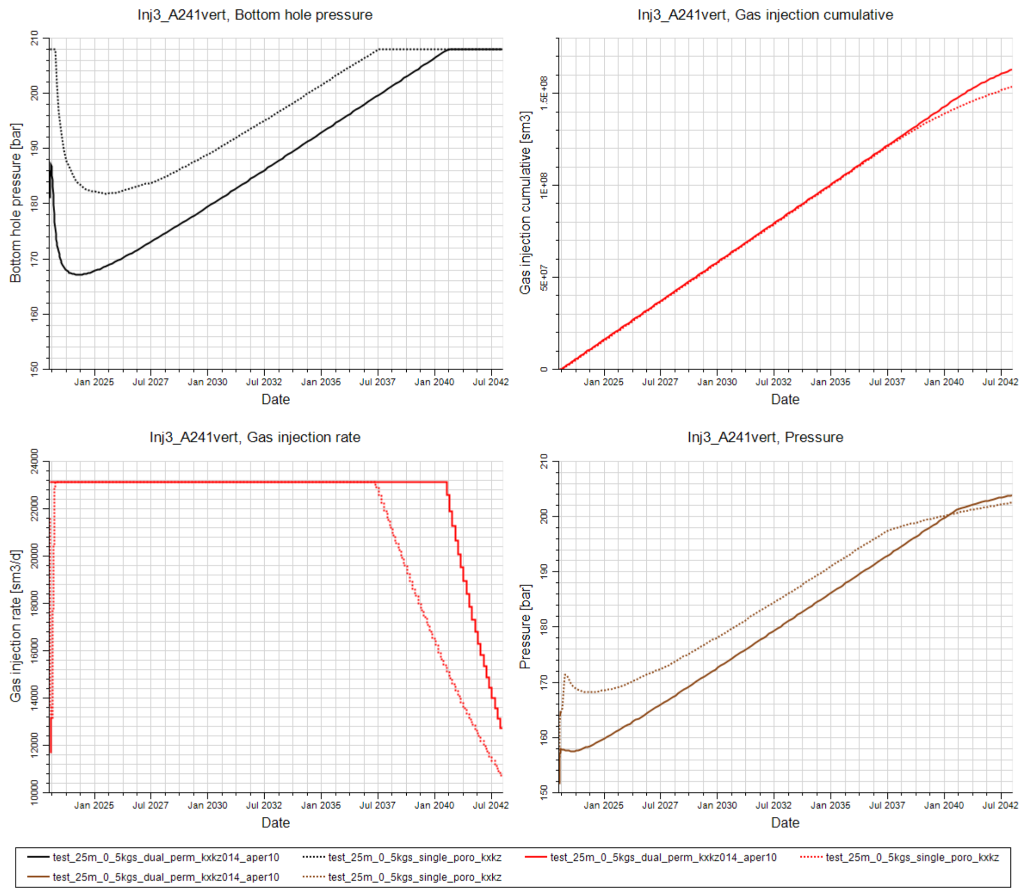

Figure 5. Diagrams of bottomhole pressure and reservoir pressure around the injection well, gas injection rate and cumulative for 20 years of continuous injection for the reservoir simulation cases 1 of single porosity (dotted lines) and 2 of dual permeability (solid lines).

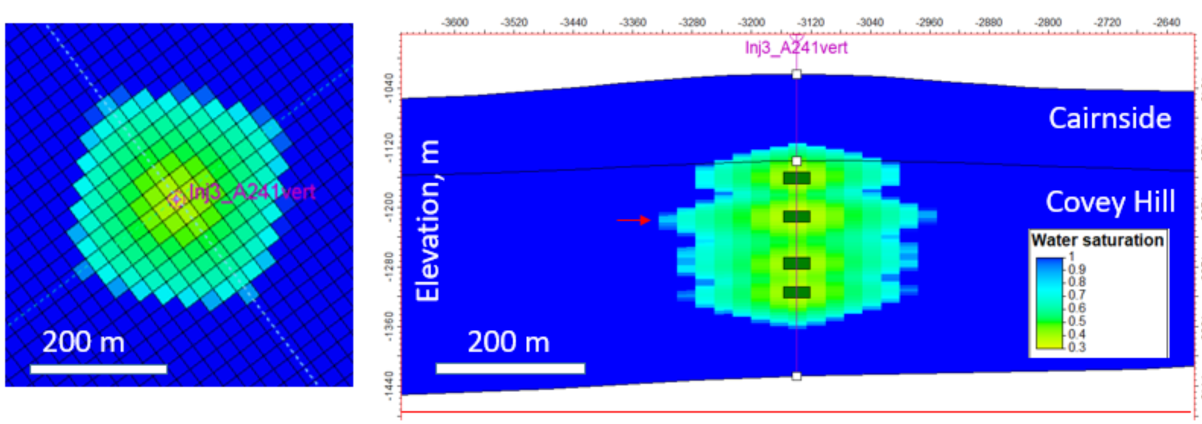

Figure 6. Map and NW-SE cross-section showing the property of water saturation after 20 years of injection for case 1 with single matrix porosity. Red arrow on the cross-section indicate depth location of the map, dashed blue line on map shows location of the cross-section.

Case 2. Dual permeability

The CO_2 injection was conducted under settings of dual permeability. To take into account the fluid flow through the fractures, the DFN modeling was performed with two fracture sets oriented Dip Azimuth

N108°/80° and N214°/80°, simplified from the results of FMI log analysis. The maximum length of fractures was set at 100 m. Fracture aperture was modeled with log-normal distribution, mean value 0.75 mm, max 5 mm. Fracture porosity was upscaled into the 3D model from DFN fracture systems (Figure 7). Fracture permeability in three dimensions was modeled using the Oda geostatistical method based on geometry and distribution of fractures in each cell (Figure 7). The transmissivity multiplier was set equal to 2.

The CO_2 was injected into the injection well at a rate of 0.5 kg/s (23117.7 Sm3/day or 15.8 kt/a), which allowed continuous injection over 17 years (Aug 24, 2040) without reaching the upper limit of the BHP of 20.8 MPa (208 bar); after that, the injection continued to Jan 2043 at lower injection rate (Figure 5). The gas injection cumulative was 304.7 kt after 20 years of injection in one well.

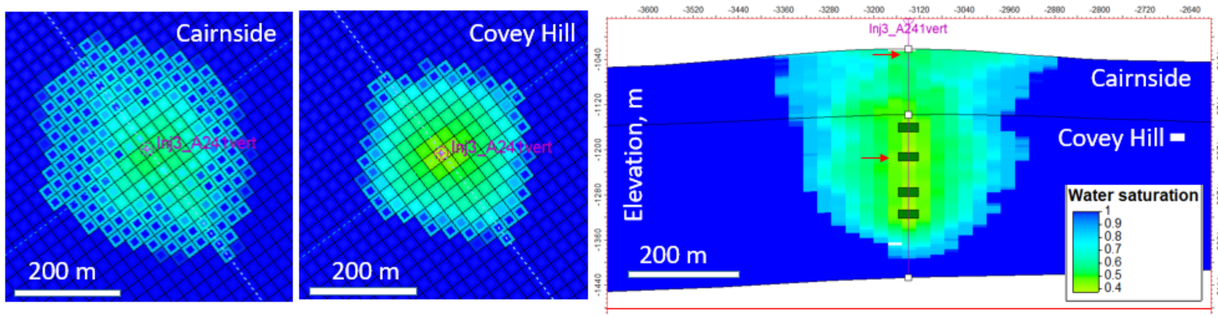

Figure 7. Maps at the top of the Cairnside Formation and in the Covey Hill Formation and NW-SE cross-section showing the property of water saturation after 20 years of injection for case 2 with dual permeability. Red arrows on the cross-section indicate depth location of the maps, dashed blue line on maps shows location of the cross-section.

The CO_2 plume was asymmetrical with a diameter of ~325 m x 350 m in the Covey Hill Formation, and it propagated through the fractures to the top of the Cairnside Formation, reaching ~400 m x 450 m in diameter at the top of the Cairnside Formation and a total height of 368 m (Figure 7).

The CO_2 injection rate applied in considered cases 1 and 2 was low (0.5 kg/s) that helps to avoid reaching the limit of the bottomhole pressure of 20.8 MPa at the top of the Potsdam sandstone and increase the risk of tensile caprock failure. The injection rate was controlled by very conservative estimation of rock matrix porosity and permeability in the Potsdam sandstone derived from log-based estimation (Figure 2). More realistically, one may expect higher porosity and permeability of the Potsdam sandstone based on the mentioned above DST data. Field tests would be required to determine safe injection rate that will not result in massive hydraulic fracturing of sandstone of the Covey Hill Formation. Additionally, DFN modeling was conducted for the Cairnside and Covey Hill Formations with similar parameters. However, these formations are characterized by different lithological composition, mechanical properties and bed thickness that result in a non-uniform fracture distribution in these units. Therefore, the upward and lateral migration of injected CO_2 might be different compared to the results obtained in case 2 (Figure 7). As fracture permeability in the subsurface is not very well constrained, simulation of CO_2 injection for cases with dual permeability with wider variability of natural fracture properties is planned.

The results of this and previous studies (Konstantinovskaya et al., 2014, 2020, 2023) support that CO_2 injection in the tight sandstone reservoir of the Potsdam Group may provide good storage capacity given considerable thickness of the sandstone and possibility of injection in multiple wells. 3D reservoir-geomechanical modeling supported by laboratory and field tests will help to increase storage volume of injected CO_2 without increasing the risk of caprock failure or shear slip fault reactivation.

Conclusions

This study made it possible to better define the storage potential of the Potsdam Group located in the industrial Bécancour area, where GHG emitters are installed.

The analysis of FMI logs in three vertical wells and one horizontal well indicates the presence of conductive, partially conductive, and resistive/healed natural fractures in the Potsdam (Cairnside) sandstone and the overlying sedimentary units. Two main sets of natural fractures were identified in the study area with mean Dip Azimuth N108°/ Dip Angle 80° and Dip Azimuth N214°/ Dip Angle 40°. The analysis of ant-tracking volume revealed the presence of discontinuity lineaments in the Covey Hill Formation, which are 480-700 m long and strike N18°E and N72°E. The first set of lineaments is parallel to conductive natural fractures identified in the image logs. However, given the relatively poor quality of the 3D amplitude volume, these data should be considered cautiously.

The 3D reservoir simulations of CO_2 injection in the Potsdam sandstone were conducted at the rate of 0.5 kg/s under the settings of single porosity (case 1) and dual permeability (case 2) to take into account the fluid flow through natural fractures. The DFN modeling of fracture systems was based on the results of the FMI log analysis. Fracture porosity and permeability were introduced into the model. Case 2 of dual permeability demonstrates better CO_2 injectivity. The borehole pressure buildup in case 2 was slower than in case 1 of single porosity. The gas injection cumulative after 20 years of injection in one well was 287.7 kt in case 1 and 304.7 kt in case 2. The CO_2 plume in case 1 was symmetrical with a diameter of 375 m and a height of 244 m; it was mainly contained in the Covey Hill Formation. The CO_2 plume in case 2 was asymmetrical with a diameter of 325 m x 350 up to 400 m x 450 m; it propagated through the fractures to the top of the Cairnside Formation with a total height of 368 m.

Results of the 3D reservoir simulations of CO_2 injection conducted in the Potsdam sandstone in the Bécancour area are being extrapolated to other industrial sectors of the St. Lawrence Lowlands, for which limited geological information is available.

Acknowledgments

The authors thank Ressources Utica Inc. for sharing the FMI data, SLB for technical support, and consolidated Petrel-Eclipse-Visage-Techlog license donation to the University of Alberta. This work is funded by CGC financial support of the OERD Program (Energy Sector) and by the Natural Sciences and Engineering Research Council of Canada (NSERC) through grants RGPIN 2019 04397 and DGECR 2019 00186.

References

Castonguay, S., J. Dietrich, D. Lavoie, and J. Y. Laliberté, 2010, Structure and petroleum plays of the St. Lawrence Platform and Appalachians in southern Quebec: Insights from interpretation of MRNQ seismic reflection data: Bulletin of Canadian Petroleum Geology, v. 58, no. 3, p. 219–234, doi:10.2113/gscpgbull.58.3.219.

Cawood, P. A., P. J. A. McCausland, and G. R. Dunning, 2001, Opening Iapetus: Constraints from the Laurentian margin in Newfoundland: Bulletin of the Geological Society of America, v. 113, no. 4, p. 443–453, doi:10.1130/0016-7606(2001)113<0443:OICFTL>2.0.CO;2.

Claprood, M., E. Gloaguen, B. Giroux, E. Konstantinovskaya, M. Malo, and M. J. Duchesne, 2012, Workflow using sparse vintage data for building a first geological and reservoir model for CO2 geological storage in deep saline aquifer. A case study in the St. Lawrence Platform, Canada: Greenhouse Gases: Science and Technology, v. 2, no. 4, p. 260–278, doi:10.1002/ghg.1292.

Girou, O., 2017, Séquestration géologique du CO2 dans les impacts hydrogéologiques potentiels à l' échelle du bassin sédimentaire: PhD Thesis. Laval University. 472 p., 472 p.

Globensky, Y., 1987, Géologie des Basses-Terres du Saint-Laurent. MM 85-02: Quebec City, 1–63 p.

Hibbard, J. P., C. R. van Staal, and D. W. Rankin, 2007, A comparative analysis of pre-Silurian crustal building blocks of the northern and the southern Appalachian orogen: American Journal of Science, v. 307, no. 1, p. 23–45, doi:10.2475/01.2007.02.

Junex inc., 2018, Saumure naturelle - Historique, ressources, réserves et perspectives de développement. Propertary report. 34p.

Konstantinovskaya, E., Q. Li, M. Malo, J. A. Rivero, M. M. Faskhoodi, and B. Campbell, 2020, Strike-slip reactivation of a high-angle normal fault induced by increase of reservoir pore pressure : insight from 3D coupled reservoir-geomechanical modeling: International Journal of Greenhouse Gas Control, v. 102, no. February, p. 103159, doi:10.1016/j.ijggc.2020.103159.

Konstantinovskaya, E., M. Malo, and D. A. Castillo, 2012, Present-day stress analysis of the St. Lawrence Lowlands sedimentary basin (Canada) and implications for caprock integrity during CO2 injection operations: Tectonophysics, v. 518–521, p. 119–137, doi:10.1016/j.tecto.2011.11.022.

Konstantinovskaya, E., J. A. Rivero, V. Vallega, J. Brodylo, and P. Coldham, 2023, 3D reservoir simulation of CO2 injection in a deep saline aquifer of the Lower Paleozoic Potsdam Sandstone of the St Lawrence Platform, Gentilly Block, Quebec: Geoenergy, v. 1, no. 1, doi:10.1144/geoenergy2022-001.

Konstantinovskaya, E., D. Rodriguez, D. Kirkwood, L. B. Harris, and R. Thériault, 2009, Effects of basement structure, sedimentation and erosion on thrust wedge geometry: An example from the Quebec appalachians and analogue models: Bulletin of Canadian Petroleum Geology, v. 57, no. 1, p. 34–62.

Konstantinovskaya, E., J. Rutqvist, and M. Malo, 2014, CO2 storage and potential fault instability in the St. Lawrence Lowlands sedimentary basin (Quebec, Canada): Insights from coupled reservoir-geomechanical modeling: International Journal of Greenhouse Gas Control, v. 22, p. 88–110, doi:10.1016/j.ijggc.2013.12.008.

Ladevèze, P., S. Séjourné, C. Rivard, D. Lavoie, R. Lefebvre, and A. Rouleau, 2018, Defining the natural fracture network in a shale gas play and its cover succession: The case of the Utica Shale in eastern Canada: Journal of Structural Geology, v. 108, no. March 2017, p. 157–170, doi:10.1016/j.jsg.2017.12.007.

Lavoie, D., 1994, Diachronous tectonic collapse of the Ordovician continental margin, eastern Canada: comparison between the Quebec Reentrant and St Lawrence Promontory: Canadian Journal of Earth Sciences, v. 31, no. 8, p. 1309–1319, doi:10.1139/e94-113.

Lewis, D. W., 1971, Qualitative Petrographic Interpretation of Potsdam Sandstone (Cambrian), Southwestern Quebec: Canadian Journal of Earth Sciences, v. 8, no. 8, p. 853–882, doi:10.1139/e71-079.

Malo, M., and K. Bédard, 2012, Basin-scale assessment for CO2 storage prospectivity in the province of Québec, Canada: Energy Procedia, v. 23, p. 487–494, doi:10.1016/j.egypro.2012.06.031.

O’Brien, T. M., and B. A. van der Pluijm, 2012, Timing of Iapetus Ocean rifting from ar geochronology of pseudotachylytes in the St. Lawrence rift system of southern Quebec: Geology, v. 40, no. 5, p. 443–446, doi:10.1130/G32691.1.

Pinet, N., 2011, Deformation in the Utica Shale and Lorraine Group , St. Lawrence Platform, Quebec: Quebec Cit, 14 p.

Ressources Utica, 2020, Data on the Chemical Composition and the Historical Production of the Becancour Hypersaline Brines Data for the Becancour #2 Well (A198). Propertary Internal Report. 8p.

Bécancour, Québec

Salad Hersi, O., and D. Lavoie, 2000, Pre-Cairnside Formation carbonate-rich sandstone: evidence for a Cambrian carbonate platform in southwestern Quebec: Ottawa, 8 p.

Séjourné, S., J. Dietrich, and M. Malo, 2003, Seismic characterization of the structural front of southern Quebec Appalachians: Bulletin of Canadian Petroleum Geology, v. 51, no. 1, p. 29–44, doi:10.2113/51.1.29.

St-Julien, P., and C. Hubert, 1975, Evolution of the Taconian Orogen in the Quebec Appalachians: American Journal of Science, v. 275- A, p. 337–362.

Tran Ngoc, T. D., R. Lefebvre, E. Konstantinovskaya, and M. Malo, 2014, Characterization of deep saline aquifers in the Bécancour area, St. Lawrence Lowlands, Québec, Canada: Implications for CO2 geological storage: Environmental Earth Sciences, v. 72, no. 1, p. 119–146, doi:10.1007/s12665-013-2941-7.

Tremblay, A., C. Sasseville, N. Clauer, and M. Zentilli, 2007, The St. Lawrence Rift System in eastern Canada—field and isotopic evidence for Paleozoic to Mesozoic (?) reactivations of Iapetus faults, *in* Geol. Soc. Am. Abstr. Programs: The Geological Society of America, Northeastern Section, p. 39(1): 95.